PETROGRAPHY OF BRITE IGNIMBRITE, TRANS PECOS, TEXAS

by 149

JERRY P. SMITH

B. S., Kansas State College, 1959

A MASTER'S THESIS

submitted in partial fulfillment of the

requirements for the degree

MASTER OF SCIENCE

Department of Geology and Geography

KANSAS STATE UNIVERSITY
Manhattan, Kansas

1967

Approved by:

Douglas M. Brookins
Major Professor

TABLE OF CONTENTS

INTRODUCTION 1

GEOLOGY 3

General Information 3

Hand Specimen Description 8

Petrographic Description 8

TERMINOLOGY USED IN THIS THESIS 9

Pyroclastic Rocks 9

Ash Flow 9

Ash-Flow Tuff 9

Ignimbrite 9

Nuee Ardente 9

THEORY OF X-RAY SPECTROGRAPHY 10

X-RAY SAMPLE PREPARATION PROCEDURE 11

Crushing and Sieving 11

Packing 11

Reliability Checks 13

PREPARATION OF STANDARD CURVES 15

General Statement 15

Counting Method 15

Ratio Method 17

Graphical Method 17

Fe_K Method 24

Errors 25

X-RAY DIFFRACTION 26

Sample Holders 26

Packing 26
DETERMINATION OF FERROUS OXIDE 30
FLAME PHOTOMETER 32
PETROGRAPHIC INVESTIGATION 38
Universal Stage Study 38
Point Counting 38
PETROGRAPHY 39
MODAL ANALYSIS OF THE BRITE IGNIMBRITE 40
Quartz Content 40
Sanidine Content 40
Anorthoclase Content 40
Matrix 43
CHEMICAL ANALYSIS OF THE BRITE IGNIMBRITE 46
SiO_2 Content 46
Al_2O_3 Content 46
Fe_2O_3 Content 46
FeO Content 58
CaO Content 58
Na_2O Content 58
K_2O Content 58
DISCUSSION 62
CONCLUSION 69
REFERENCES CITED 71
ACKNOWLEDGMENTS 73
APPENDIX 74
X-ray Tube Selection 75

Crystal Selection 75

Table of Analyzing Crystals 77

X-ray Spectrographic Specifications 79

Analyses of Standard Rock Powders 84

Reagents and Solutions for the Determination of Ferrous Oxide . . . 88

LIST OF ILLUSTRATIONS

Figure

1. Sample Location Map 5

2. Aerial View of Cuesta del Burro 7

3. Standard Curves for SiO_2 and Al_2O_3 19

4. Standard Curves for Total Fe and FeO 21

5. Standard Curves for CaO and K_2O 23

6. X-ray Diffraction Patterns of Whole-rock and Sanidine Feldspar . . 29

7. Flame Photometer Standard Curves for Na_2O and K_2O 35

8. Photomicrograph of Ignimbrite Showing Relict Structures of Pre-existing Texture 66

LIST OF TABLES

Table

1. Oxide Percentages of Na_2O and K_2O by Flame Photometry 37
2. Mineralogic Composition from Point Counts 42
3. Percent SiO_2 in Glass of Matrix by Index of Refraction 45
4. Original Chemical Data 48
5. Normalized Chemical Data 51
6. Niggli Molecular Normative Data 54
7. Titration Data for FeO 60
8. Table of Analyzing Crystals 77
9. Table of K Peak Angles 79
10. Table of K Peak Angles 81
11. Oxide Analyses of Standard Rock Powders 84

INTRODUCTION

Geochemical data on volcanic rocks, and especially ignimbrites, are sporadically distributed throughout the existing literature and somewhat restricted in scope. A particular problem is the lack of analytical control during the accumulation of some of the data; and, more serious, often only meager attempts to correlate the chemical data with petrographic and X-ray studies.

This study has been undertaken with two prime purposes in mind: (1) to carefully test various analytical methods suitable for obtaining data from ignimbrites, and (2) to interpret these data in the light of contemporaneous petrographic and X-ray diffraction investigations. No broad geologic interpretations from the results of this study are intended; and, indeed, the samples selected for this study (described later) were donated from the collection of Dr. Page C. Twiss (Geology Department, KSU). It is hoped, however, that the data will contribute towards a better understanding of the ignimbrite problem.

The Brite Ignimbrite (Davis Mountains Volcanic Province; terminology following Smith, 1960) was selected for study because: (1) it is widely distributed, (2) some previous detailed work has been done on it (Twiss), and (3) numerous samples were available for study. The Brite Ignimbrite will be discussed in more detail in a later section.

Analyses were made on each sample for the major elements present in the rock, using X-ray spectrography, flame photometry and analytical chemistry. In addition, each sample was point counted to obtain the mineralogic composition and to facilitate the calculation of CIPW norms. The data resulting from these analyses are presented in terms of the oxide percentage of

each major element and as normative percentages of each mineral. This allows the data to be readily compared to rocks from any other volcanic province.

The term ignimbrite as used hereafter in this paper refers to any and all extrusive rocks of pyroclastic origin, whether deposited from a nuee ardente or from an ash flow (terms defined later).

The term "snowflake" to indicate the texture of a devitrified matrix (Twiss, written communication) is used in the text of this paper.

GEOLOGY

General Information

The Brite Ignimbrite is the most laterally continuous and widely distributed volcanic flow in Trans-Pecos Texas. Its entire surface exposure has not yet been completely mapped, but is known to be exposed over an area of more than 3000 square miles in Texas and Chihuahua, Mexico. Due to its lateral continuity and large area of exposure, it is used as the principal stratigraphic marker for the area (Twiss, oral communication). In addition, the Brite Ignimbrite is laterally continuous with the Mitchell Mesa Rhyolite which has been studied by Tuttle and Bowen (1958).

The Brite Ignimbrite is a member of the Vieja Group (of Tertiary Age) and it ranges in thickness from near 0 to approximately 300 feet. The relationship of the Brite Ignimbrite to the other members of the Vieja Group has been described by Twiss (written communication) (see Figure 1 for sample locations).

The most prominent topographic features in the area are the Bute Rim and Cuesta del Burro; both are a north trending escarpment formed by a faults with approximately 1000 feet vertical displacement. Both features are capped by the Brite Ignimbrite.

The Brite Ignimbrite dips to the east over most of the area, and its surface exposure is interrupted only by several major north trending faults and numerous smaller intersecting faults. A typical view of the Brite Ignimbrite is shown in Figure 2, which shows a view looking north along Cuesta del Burro, and which emphasizes the prominence of the escarpment above the surrounding, comparatively monotonous terrain. Several of the smaller intersecting faults are also evident in Figure 2.

EXPLANATION OF FIGURE 1

Location of samples of Brite Ignimbrite.

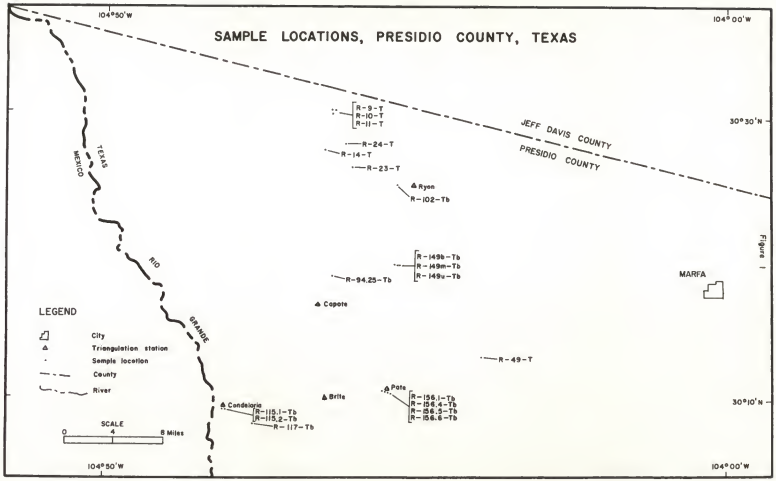
SAMPLE LOCATIONS, PRESIDIO COUNTY, TEXAS
104°50'W
104°00'W
30°30'N
30°10'N
JEFF DAVIS COUNTY
PRESIDIO COUNTY
TEXAS
MEXICO
RIO GRANDE
MARFA
Figure 1
R-9-T
R-10-T
R-11-T
R-24-T
R-14-T
R-23-T
Ryon
R-102-Tb
R-149b-Tb
R-149m-Tb
R-149u-Tb
R-94.25-Tb
Coyote
R-49-T
Brite
Pote
R-156.1-Tb
R-156.4-Tb
R-156.5-Tb
R-156.6-Tb
Candelaria
R-115.1-Tb
R-115.2-Tb
R-117-Tb
LEGEND
City
Triangulation station
Sample location
County
River
SCALE
0
4
8 Miles

Figure 1

EXPLANATION OF FIGURE 2

Aerial view of Cuesta del Burro.

Figure 2

Hand Specimen Description

In hand specimen the Brite Ignimbrite ranges from light olive gray ($5Y\frac{7}{1}$) (Twiss, written communication) to light brownish gray ($5YR\frac{6}{1}$) in groundmass and it weathers to light brown ($5YR\frac{6}{4}$) groundmass with the chatoyant sanidine phenocrysts standing out in high relief because of their resistance to erosion.

The phenocrysts consist of small, angular, clear quartz grains and chatoyant, tabular feldspars approximately 4mm long. The overall texture is hypocrystalline.

Petrographic Description

Phenocrysts of subhedral to enhedral crystals of quartz and feldspar are enclosed in a granophyic "snowflake" matrix of alkali feldspar and quartz with minute hairs of brown volcanic glass (refractive index 1.52). The color of the brown volcanic glass can be attributed to concentrations of finely disseminated Fe_2O_3 within it. A few miarolitic cavities containing quartz, calcite and alkalic feldspar are evident. The most prevalent accessary mineral is lamprobolite, which occurs as traces and in some cases shows alteration rims of biotite.

Previous studies on the Mitchell Mesa. Rhyolite (Deford, 1958; Tuttle and Bowen, 1958) which is laterally continuous with the Brite Ignimbrite, show an Or content of 44% for the bulk composition of the rock. For the separate K and Na phases, Or-92 and Or-0 (respectively) have been reported. Erickson (1953) has reported a 2V 40^{o} for the K-feldspar, and this figure coupled with the above composition places the K-feldspar intermediate between sanidine and anorthoclase (although probably closer to anorthoclase).

TERMINOLOGY USED IN THIS THESIS

The following definitions are taken from Ross and Smith (1960):

Pyroclastic Rocks

Pyroclastic rocks are a transitional group, composed of lava fragments, but which are laid down generally like sediments.

Ash Flow

A turbulent mixture of gas and pyroclastic materials of high temperature, ejected explosively from a crater or fissure, that travels swiftly down the slopes of a volcano or along the ground surface. The solid material in an ash flow, although unsorted, is dominantly of particles of ash size (less than 4mm in diameter) but generally contains different amounts of lapilli and blocks.

Ash-flow Tuff

The consolidated deposits of volcanic ash resulting from an ash flow, which may or may not be completely or partly welded.

Ignimbrite

Marshall (1935) proposed the name "ignimbrite" (literally fiery rain cloud rock). This is interpreted to mean a rock of "acid composition" formed by the fall from a cloud of hot viscous material.

Nuee Ardente

Lacroix (1903a) proposed the term to describe an eruption made up of an emulsion of solid material in a mixture of water vapor and gas at high temperature.

THEORY OF X-RAY SPECTROGRAPHY

X-ray spectrography (often referred to as X-ray flourescence) is a non-destructive method of analyzing a material qualitatively and quantitatively for its elemental composition.

Each element will emit characteristic X-radiations when excited by a source of shorter wavelength and sufficient power to excite the inner shell electrons to a higher energy state. As the electrons fall back to their "at rest" state, they "flouresce" or emit X-radiations. These X-radiations are detected and recorded.

In actual practice, a sample is bombarded by an X-ray source and each element in the sample emits its characteristic X-radiations. These X-radiations are focused on an analyzing crystal of known interplanar spacing. The X-radiation of each element, depending on its characteristic wavelength ($\AA$) and the interplanar spacing (2D) of the analyzing crystal, will be diffracted upon entering the analyzing crystal according to the Bragg equation:

$$n = 2D \sin \theta$$

Therefore, the characteristic X-radiation from each element can be detected by scintillation or geiger counters as a scan across the spectrum is made.

The intensity of each characteristic X-radiation is directly proportional to the concentration of the excited element.

For a more detailed account of the theory of X-ray the reader is referred to Birks (1964), Klug and Alexander (1954) and Smales and Wager (1960).

X-RAY SAMPLE PREPARATION PROCEDURE

Crushing and Sieving

The first step consists of crushing and sieving the samples to the required grain size. This required size will be determined by the accuracy and reproducibility desired. For rapid determinations of major constituents, without extreme accuracy, crushing and sieving the samples to a size of minus 120 mesh is quite sufficient. However, when maximum accuracy is of primary concern, it is recommended that all samples be crushed to minus 230 mesh.

If iron contamination is of little concern, most samples can be crushed in a steel mortar and pestle, followed by a final grinding in an agate mortar and pestle. This procedure is quite rapid if large quantities are not needed.

If maximum accuracy in the iron determinations is needed, it becomes necessary to grind the samples in an agate mortar and pestle only or tungsten carbide mill.

Packing

In order to insure maximum sample density and uniform packing, each sample is packed into specially designed sample holders immediately before insertion into the X-ray spectrograph. These sample holders are green fiberglass cylinders, 32mm in outside diameter. A recess, 25mm in diameter and 4mm deep, is milled into one end to act as a sample cup.

Care must be taken that each sieved sample is thoroughly mixed until it is homogenous so that any aliquot removed for packing will be representative of the whole.

Enough sample is poured into the sample holder to make a small mound. After pressing as much of the powder as possible into the holder with a spatula, a clear glass petrographic slide is used to further pack the powder. It is of utmost importance that the powder be as tightly packed as possible. This will vary accordingly with the fineness of the powder because poorly sorted, coarse fractions are difficult to pack properly. In general the tighter a sample is packed, the higher the intensity of each element peak.

Ideally after packing, the individual crystallites in a sample should be randomly oriented with respect to the incident X-ray beam. The average sample will be oriented to a degree depending on the physical shape of each individual crystallite.

Samples that have a prominent cleavage should be ground in such a manner that this feature is minimized. The techniques used for grinding samples for oil immersion work are useful for this situation (i.e. percussion crushing versus grinding).

The very minimum test that a sample must pass after packing is to turn the holder upside down to see if the powder is self supporting and does not fall out of the holder under its own weight. If it will support its own weight it is ready for insertion into the aluminum sample holders provided with the X-ray spectrograph.

The final test to determine if a sample has been ground sufficiently and well packed, is to obtain the corrected intensity values for a peak or series of peaks. Then remove the powder from the holder, repack it and repeat the determination. If the reproducibility is not within the desired limits of accuracy, attention should first be given to the uniformity of packing between runs. Care in packing should eliminate any gross errors

between successive runs. If most of the sample is greater than 230 mesh, the next step to obtain greater reproducibility is further grinding.

Any other errors in accuracy, assuming all instrument settings are held constant, can be attributed to instrument drift with time or to the error in locating the exact maximum of the peak, the proper background correction, or both.

Reliability Checks

As a check on machine electronics drift, errors associated with packing and any other non-random fluctuations in the analyses, each sample should be removed from its holder and repacked. A sufficient number of determinations are made for each element desired in each sample to insure that the best average intensity possible has been obtained. Under normal conditions three separate runs will be adequate, assuming that each sample was repacked prior to the run. Also, between every few unknowns, a reliable standard should be analysed so that any systematic error (primarily due to machine electronic fluctuations) can be corrected.

Another, and possibly more dependable check on machine electronic fluctuations, which are primarily due to changes in the effective output of the X-ray tube source, is to use a silicon wafer, copper sheet, or some other element near the range of the element being analysed. This checking is done by first determining the intensity of some standard (i.e. the copper sheet) at one well-defined and easily reproducible 2θ angle. This will normally be a quite high intensity relative to an unknown and will necessitate some switching of the scale factor. However, any major deviations from this original intensity can be readily noticed. Should the output vary

more than a few percent, it can be brought back to its original intensity by increasing or decreasing the current applied to the X-ray tube.

PREPARATION OF STANDARD CURVES

General Statement

There are several acceptable methods for obtaining and portraying the data using the X-ray spectrograph, four of which will be described in the following pages. These are the (1) Counting Method, (2) Ratio Method, (3) Graphical Method and the (4) Fe_K Method. Each of these methods are valid in theory and use, varying only in the manner in which the data will be collected, the source of errors involved, time available to complete the analysis and the physical units the operator prefers to use.

It is important to note, at this time, that the final success and accuracy of any method directly depends upon the diligence and consistency of the operator. This applies, not only to sample preparation and packing, but, to each instrument setting no matter how trivial it might appear.

Counting Method

The Counting Method is probably more accurate than any other method, providing proper application is rigidly followed.

There are two modes of operation in the Counting Method. These are Fixed Time and Fixed Count and are selected for ease in presenting the data. When using the Fixed Count mode, the values for peak intensity and background are in terms of time per set number of counts. This usually necessitates some recalculation, to the more meaningful, counts per second. Although this is a simple mathematical calculation it can become laborious. Therefore, it is suggested that the Fixed Time mode be used for most routine analyses. In the Fixed Time mode, an instrument setting is used to allow a sufficient number of counts to be recorded, such that the standard deviation

of that number of counts is less than or equal to the required accuracy.

A scan across the desired peak is recorded to ascertain the exact location of the 2θ angle for the maximum intensity of the peak and the 2θ angles for the average background on each side of the element peak. The goniometer settings can now be determined, which will provide average background intensities and the maximum intensity for the element. At each of these points, the intensity in counts per second is determined. The average background intensity at the peak is calculated and subtracted from the average peak intensity. This results in a value in counts per second that is proportional to the concentration of the element.

Standard curves are established by using samples with known concentrations of the desired element in terms of their oxides or elemental units (such as parts per million). Standard powders of analyzed rocks are available (see Appendix) which are similar in overall characteristics such that any significant differences, between their mass absorption coefficients and those of the unknowns, are held at a minimum.

A standard curve is plotted for each element using several standard rock samples for which the concentration of the desired element is known and for which corresponding intensity values have been determined X-ray spectrographically. The concentration of the element is usually plotted as the abscissa and the intensity as the ordinate on the resulting graph. Several points are needed to accurately establish the shape of the curve. It is highly preferable that the span between the standards be large enough to permit the interpolation of the unknowns rather than necessitating extrapolation. Extreme caution and judgement must be exercised before accepting any determinations that fall beyond the limits of the standards. This is

necessitated because of matrix effects such as differences in the mass absorption coefficients between the standards and the unknowns (see Figures 3 through 5 for examples of standard curves).

Ratio Method

The reader is referred to the excellent detailed discussion of Fairbairn (1966) for the procedures of this method.

Graphical Method

The Graphical Method was used for the X-ray spectrographic analyses reported in this investigation. This method is simple and straightforward.

It is permissible to determine the peak intensity and average background directly from a scan made across an element peak, since the output of the X-ray spectrograph used is linearly proportional to the input.

In utilizing this method, it is advisable to use the same instrumental settings for as many of the determinations as possible. The Norelco X-ray spectrograph contains a built-in time constant in the rate-meter which varies inversely as the scale factor. For this reason, it is necessary to lower the setting of the time constant as the scale factor is increased. This manipulation minimizes any inherent differences between the time constants of the different scales.

The intensity of the desired peak is the difference between the percentage of full scale deflection less the average background under the peak. It is essential that the maximum intensity of the peak and the background be determined at the same 2θ angles for each sample. Enough determinations are made for each standard and unknown such that any deviations from the true value will be minimized.

EXPLANATION OF FIGURE 3

Standard curves for SiO_2 and Al_2O_3. Instrument settings—SiO_2, chromium target, 50kvp, 23ma, PET crystal, L = 10.0v, W = 14.0v, detector = 1.64kv; Al_2O_3, chromium target, 50kvp, 23ma, PET crystal, L = 7.0v, W = 13.0v, detector = 1.64kv.

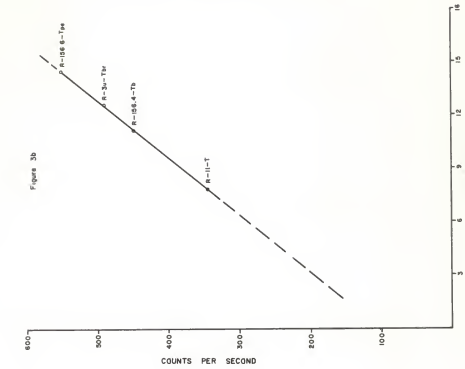
Figure 3b
R-156 B-Tpx
R-3a-Thr
R-156.4-Tb
R-11-T
COUNTS PER SECOND
Wt. % Al_2O_3

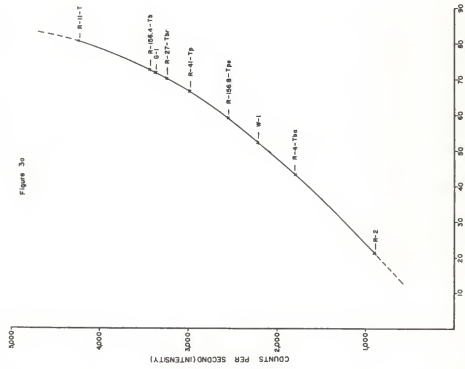
Figure 3a
R-11-T
R-156.4-Tb
R-27-Thr
R-41-Tp
R-156 B-Tpx
W-1
R-4-Thx
R-2
COUNTS PER SECOND (INTENSITY)
Wt. % SiO_2

EXPLANATION OF FIGURE 4

Standard curves for total Fe and FeO. Instrument settings--Total Fe, Molybdenum target, 50kvp, 40ma, Topaz crystal, L = 6.0v, W = 10.0v, detector = 0.98kv; FeO, see Appendix.

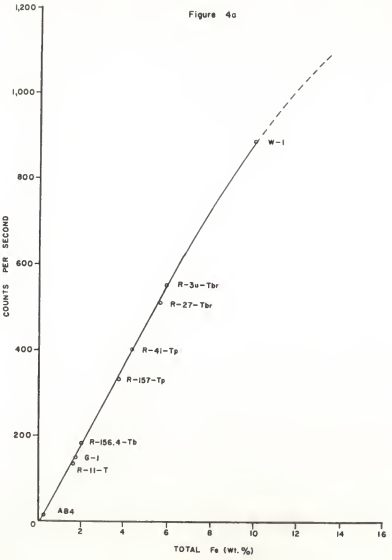
Figure 4a
1,200
1,000
800
600
400
200
0
COUNTS PER SECOND
W-1
R-3u-Tbr
R-27-Tbr
R-41-Tp
R-157-Tp
R-156.4-Tb
G-1
R-11-T
AB4
2
4
6
8
10
12
14
16
TOTAL Fe (wt. %)

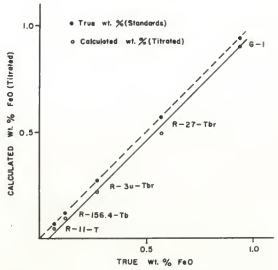
Figure 4b
• True wt. %(Standards)
o Calculated wt. %(Titrated)
1.0
0.5
CALCULATED WT. % FeO (Titrated)
G-1
R-27-Tbr
R-3u-Tbr
R-156.4-Tb
R-11-T
0.5
1.0
TRUE wt. % FeO

EXPLANATION OF FIGURE 5

Standard curves for CaO and K_2O. Instrument settings--CaO, chromium target, 50kvp, 23ma, PET crystal, L = 13.0v, 12.0v, detector = 1.56kv; K_2O, chromium target, 50kvp, 23ma, PET crystal, L = 7.0v, W = 13.0v, detector = 1.56kv.

Figure 5a

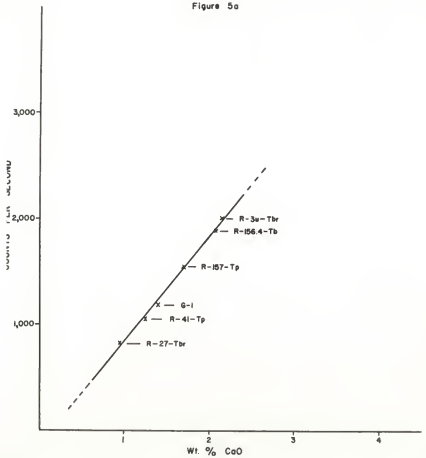

Figure 5b

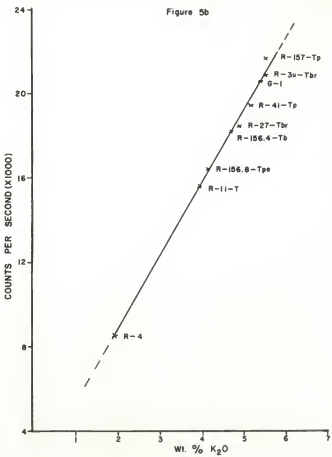

Fe_K Method

One of the problems in measuring the concentration of an element by the X-ray spectrograph is the absorption effect of heavy elements in the matrix. Of the eight most abundant elements in crystalline rocks, iron (Fe^{++} and Fe^{+++}) is the heaviest. The photons of energy present in the X-ray beam are directed on the sample and are absorbed to a greater degree by iron than by any of the other major elements. Any correction that is made for the effect of absorption tends to bring the experimental data closer to the true concentration of the element in a sample.

The general principle of measuring the concentration of an element, using the Fe_K method, by the X-ray spectrograph is as follows:

$$Z_{int.} = k(Z_{conc.}) \quad \text{and} \quad k = \frac{Z_{int.}}{Z_{conc.}}$$

where $Z_{int.}$ is the average corrected intensity of a sample, $Z_{conc.}$ is the concentration of the element in the unknown or standard samples. The value of k depends on many variables; such as particle size, packing, sample holder composition, matrix effect and others. The effect of all of the variables except the matrix effect can be controlled or minimized by strictly following the same procedures for both standards and unknowns. The matrix effect is independent of the procedures, but a correction factor can be calculated from the curve established by the above equation, which takes into consideration the effect of the iron absorption or flourescence.

For each element to be determined it is necessary to plot a working curve of the concentration of the element versus the Fe_K intensity.

Errors

The error about any one or set of determinations can be determined by the following equation:

$$t = \frac{T}{N^{\frac{1}{2}}} ,$$

where t is the standard deviation of T, which is the time needed to collect N counts. Excellent discussions on the computation of the statistical data are presented in Smales and Wager (1960) and Birks (1959).

X-RAY DIFFRACTION

The samples used for X-ray diffraction analysis were aliquots of those used for X-ray spectrographic analysis.

Sample Holders

The sample holders consist of 35mm x 38mm x 1mm aluminum sheet with a rectangular opening, 10mm x 20mm, near one end.

Packing

The powdered rock sample was poured into the opening in the sample holder, which is placed upside down on a glass plate. The powder was lightly packed with a petrographic slide and any excess scraped off. A 22mm glass cover slip was taped to the back of the sample and holder and the complete mount turned over. This method insures a smooth sample surface without extreme particle alignment. The reproducibility was entirely satisfactory for qualitative determinations.

X-ray diffractometer patterns were obtained for each whole rock sample available and for one nearly pure sanidine fraction of one sample. These diffractometer patterns were made from 62 degrees 2θ to 0 degrees 2θ at a rate of 1 degree per minute to determine the bulk mineralogy.

The bulk mineralogy so determined proved to be uniform throughout the samples, varying only in the percentages of the individual minerals present.

Minerals present in detectable quantities are: quartz, secondary calcite (some dolomite), and feldspar. The feldspar in the samples consists of high sanidine, high Albite and anorthoclase.

A portion of a typical whole-rock X-ray diffraction pattern is shown in Fig. 6b. This X-ray diffractometer pattern shows sanidine, anorthoclase and

sodic-calcic plagioclase in the whole-rock mass.

Figure 6a is the X-ray diffractometer pattern of feldspar which was handpicked from sample R-156.4-Tb. All of the feldspar was chatoyant. The contamination from the groundmass is less than 5 percent of the total volume. This groundmass material probably accounts for most of the quartz peak intensity, however. It is evident from this pattern that a member of the sanidine-anorthoclase series, and sodic-calcic plagioclase are in the separate as well as in the whole-rock. This is further confirmation of the partial inversion of the sanidine to orthoclase cryptoperthite (or X-ray perthite) (see Tuttle and Bowen, 1958). Further detailed work at a later date will be necessary to ascertain the true identity and composition of these feldspars.

EXPLANATION OF FIGURE 6

Figure 6a is the whole-rock X-ray diffractometer pattern of sample R-115.2-Tb.

Figure 6b is the X-ray diffractometer pattern of the sanidine fraction from sample R-156.4-Tb.

No significant mineralogical differences in the patterns is apparent. This indicates no appreciable differences in the mineralogy of the matrix and phenocrysts.

Figure 6a
Scale factor ×1,000
4.26Å Quartz
4.03Å Albite
3.98Å Anorthoclase
3.77Å Anorthoclase
3.19Å Albite
3.48Å Anorthoclase
3.43Å Sanidine
3.24Å Quartz
3.20Å Sanidine
3.20Å Anorthoclase
2.98Å Anorthoclase
2.89Å Sanidine
2.76Å Sanidine
2.61Å Sanidine
2.57Å Sanidine
Figure 6b
Scale factor × 500
Unresolved halogen peak
4.03Å Albite
3.85Å Sanidine
3.75Å Sanidine
3.45Å Sanidine
3.34Å Quartz
2.98Å Anorthoclase
2.99Å Sanidine
2.79Å Sanidine
2.96Å Albite
2.36Å Albite
2.26Å Sanidine
20°
24°
28°
32°
36°

DETERMINATION OF FERROUS OXIDE

FeO was determined using the method outlined by Peck (1964).

1. A 0.5000 gram aliquot of each sample used for X-ray spectrographic analysis was transferred to a 30ml platinum crucible. One ml of demineralized water was added to form a slurry.
2. A lighted bunsen burner and shielded tripod were placed under a well-ventilated hood. The flame was adjusted to approximately one-half inch in height (minimum necessary to sustain a slow boil).
3. Five ml of demineralized water and 5ml of 48% hydroflouric acid were added to a graduated cylinder and 5ml of concentrated sulfuric acid was added to a second graduated cylinder.
4. The sulfuric acid is slowly added to the slurry in the platinum crucible and followed by the addition of the water and acid mixture.
5. A tight-fitting platinum lid with a small hole in its center is used to cover the crucible and the assembly is placed on the tripod. The crucible is heated until a continuous flow of steam issues from the hole in the cover. Continue heating for an additional 10 minutes.
6. During this 10-minute interval, 100ml of "dissolving solution" (see Appendix for preparation of reagents) is added to a 600ml Pyrex beaker. This "dissolving solution" is then diluted to 300ml and two drops of 0.2 percent sodium diphenylamine sulphonate indicator are added.
7. After the 10-minute heating period, the crucible is removed from the tripod with a pair of tongs; the Pyrex beaker is tipped forward and the crucible is lowered into it until the bottom is immersed in the liquid. Then, the crucible is released and allowed to sink into the solution. With the aid of a stirring rod, the crucible and its cover is lifted

from the Pyrex beaker; washed thoroughly with water and set aside.

8. The solution is titrated, while stirring, with 0.06262N potassium dichromate solution until the purple color caused by the addition of one drop of the titrant fades slowly. Continue adding the titrant until the purple color persists for 30 seconds.

9. Calculations:

   Milliliters $K_2Cr_2O_7$ x 0.9 = percent FeO.

FLAME PHOTOMETER

The flame photometer was used for the determination of Na_2O and K_2O in each of the samples.

An aliquot (0.2gm) of each sample was dissolved using 10ml of perchloric acid. This mixture of acids and sample was evaporated without boiling in 100ml teflon dishes to near dryness. Ten ml of 6N hydrochloric acid was then added to the residue; and this mixture was slowly heated until the residue was again dissolved. This solution was transferred to a 200ml volumetric flask. Twenty milliliters of 0.1% lithium chloride solution (reagent grade) was then added (to provide a standard base for the flame photometer) and the contents were diluted to 200ml.

For each element to be determined by flame photometry, standard solutions are prepared containing that element in known concentrations. These solutions are prepared with a range of concentration such that hopefully most of the unknowns will fall at approximately 80% of the maximum standard concentration.

To each standard and unknown solution, 100ppm lithium ion must be added as an internal standard.

The following formula is used to determine the volume of each standard solution necessary to give the desired ionic concentration:

$$\frac{V_x}{V_y} = \frac{C}{Z}$$

where V_x is the volume of standard to be added in milliliters, V_y is the total volume of the standard, C is the concentration in parts per million in the sample and Z is the concentration (in parts per million) of the standard

solution.

After the necessary ions are added, the solutions are brought up to their desired volumes with demineralized water.

The internal standard readings for each standard are determined and plotted versus the concentration (see Fig. 7).

The analyses for Na_2O and K_2O by flame photometry are summarized in Table 1.

EXPLANATION OF FIGURE 7

Flame photometer standard curves for Na_2O and K_2O.

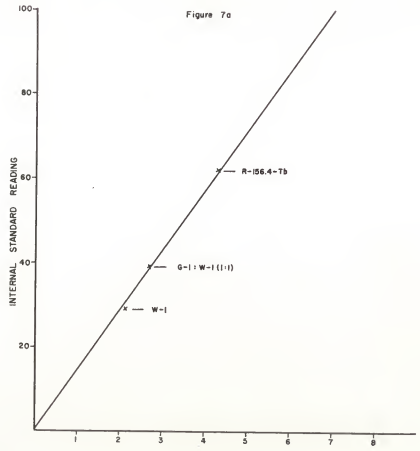
Figure 7a
INTERNAL STANDARD READING
100
80
60
40
20
1
2
3
4
5
6
7
8
R-156.4-Tb
G-1 : W-1 (1:1)
W-1

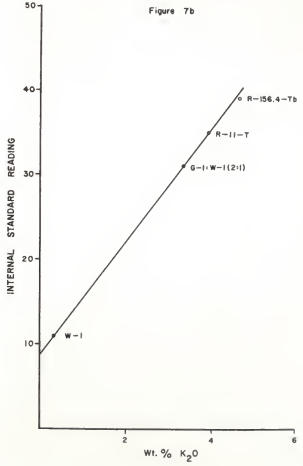
Figure 7b
INTERNAL STANDARD READING
50
40
30
20
10
2
4
6
Wt. % K_2O
R-156.4-Tb
R-11-T
G-1 : W-1 (2:1)
W-1

EXPLANATION OF TABLE 1

Oxide percentages of Na_2O and K_2O by flame photometry.

TABLE 1

Flame Photometer Data

Sample	Wt. % Na_2O	Wt. % K_2O
R-9-T	2.40	4.50
R-10-T	2.46	4.06
R-11-T	3.03	3.99
R-23-T	1.36	4.29
R-24-T	2.29	3.99
R-49-T	4.04	5.20
R-94.25-Tb	2.47	3.65
R-102-Tb	2.35	3.68
R-115.1-Tb	3.50	5.95
R-115.2-Tb	4.16	4.76
R-117-Tb	3.69	4.13
R-149b-Tb	2.81	5.65
R-149m-Tb	3.49	5.65
R-149u-Tb	3.46	5.04
R-156.1-Tb	4.08	4.74
R-156.4-Tb	4.41	4.60
R-156.5-Tb	2.00	2.76
R-156.6-Tb	2.13	3.38
R-161-Tb	6.60	
G-1	3.29	5.52
G-1:W-1 (1:1)	2.72	3.08
W-1	2.15	0.63

PETROGRAPHIC INVESTIGATION

Universal Stage Study

In the early stages of this investigation, an attempt was made to identify the composition of the feldspars from their optic angles (2V) using the universal stage. The method employed has been described in detail by Haff (1942).

A wide range of values ($2V=18^{o}$ to $2V=58^{o}$) were obtained for each specimen examined. For this reason, no significant values can be used to determine the composition of the feldspars. Tuttle and Bowen (1958) stated that these variations in the optic axis angle are probably a result of partial inversion of sanidine to orthoclase cryptoperthite (or X-ray perthite). This is probably a valid assumption and is better illustrated in the section on X-ray Diffraction.

Point Counting

The thin-sections cut from each sample were point-counted according to the straight counting method described by Chayes (1956). A rectangle, 1 inch x 3/4 inch, was inked on each slide and approximately fifteen hundred points were counted. The counts were taken at 1mm intervals in each row with 0.3mm between the rows. One of the corners of the rectangle was selected as the starting point of the first traverse with each alternate traverse being taken in the reverse direction. The unique point under the microscope cross-hair was recorded for each interval of the traverse. The total number of counts for each mineral in the slide was ascertained and recalculated to percent of the total.

PETROGRAPHY

In thin-section the Brite Ignimbrite is remarkably uniform in texture and composition. The phenocrysts (10% to 20% of the total volume) consist of subhedral to enhedral crystals of quartz and alkali feldspar. These are surrounded by a granophyric matrix of microscopic quartz and alkali feldspar with minute hairs of brown volcanic glass (of refractive index 1.52). The brown color of the volcanic glass can be attributed to concentrations of finely disseminated Fe_2O_3 within it.

The overall texture is hypocrystalline. Sanidine phenocrysts up to 4mm long constitute approximately 12% of the total amount, and quartz up to 2mm long 5%.

Lamprobolite, biotite, iddingsite, magnetite and hematite are accessory minerals in most samples. Siltstone and ignimbrite fragments are also in a few samples. Biotite, when present, usually forms alteration rims surrounding the lamprobolite.

Secondary calcite ranging up to 5% is in most samples. This calcite is generally finely disseminated throughout the matrix except where in a few samples it fills vesicles.

The few miarolitic cavities observed are believed to contain cristobalite and alkali feldspar. The alternating cristobalite and alkali feldspar microcrystallites are axiolitic within the cavities.

MODAL ANALYSIS OF THE BRITE IGNIMBRITE

Modal analyses were made on 12 specimens (see Table 2) using the straight counting method described by Chayes (1956). The results from these point counts did not justify further investigation by this method. Each analysis was made by traversing across a thin section and identifying the mineral at the intersection of the crosshair at 1mm intervals. The traverses were spaced 0.3mm apart with alternating traverses made in opposite directions.

Quartz, sanidine, anorthoclase, matrix (including glass) were recorded separately; and the other constituents were lumped together.

Quartz Content

Of the 12 specimens studied by the point count method, the quartz content ranged from 0 to 8.66 percent; the average quartz content was 1.38 percent.

Sanidine Content

Sanidine is the most abundant mineral in the specimens examined; it ranges from 7.47 percent to 19.57 percent; the average sanidine content is 12.33 percent. The sanidine is subhedral to enhedral with blebs of glass incorporated within the phenocrysts indicating their partial resorption.

Anorthoclase Content

Anorthoclase was noted in only 4 of the 12 specimens examined. The anorthoclase content for these 4 specimens ranged from 0.20 percent to 5.16 percent.

EXPLANATION OF TABLE 2

Mineralogic composition from point counts.

TABLE 2

Mineralogic Composition from Point Counts

Sample	Matrix	Sanidine	Anorthoclase	Quartz	Other	Total
R-9-T	83.52	12.89	2.52		1.06	99.99
R-10-T	89.47	8.85		0.13	1.52	99.97
R-11-T	83.55	13.56		0.98	1.90	99.99
R-14-T	81.85	14.74			3.43	100.02
R-49-T	84.53	12.86	1.81		0.80	100.00
R-94.25-Tb	79.88	12.97	0.20		6.96	100.01
R-102-Tb	91.41	8.07		0.07	0.45	100.00
R-117-Tb	75.96	13.72		8.66	1.70	100.04
R-156.1-Tb	82.03	15.10		1.94	0.94	100.01
R-156.4-Tb	78.14	19.57		1.69	0.60	100.00
R-156.5-Tb	90.37	8.14		0.66	0.86	100.03
R-156.6-Tb	82.55	7.47	5.16	2.37	2.45	100.00

Matrix

The greatest variability in the modal analyses of the Brite Ignimbrite can be attributed to the composition of the matrix. The texture of the matrix shows typical and distinctive flow structures, commonly reported from ignimbrites, in only a few of 20 specimens studied. The flow structures, where present, appear to be much less pronounced than in the photomicrographs used for illustration of typical ignimbrites by Ross and Smith (1960). In most of the specimens studied, this flow structure was missing entirely, incomplete, or very indistinct.

It is not known from which zone of welding a particular specimen was collected, and any differences in the texture might be due to the different degrees of welding.

The matrix exhibits a granophyric texture with a few inclusions of siltstone and ignimbrite fragments. These fragments also show a granophyric texture with only the relict structure of the original fragments remaining. This suggests, and it is here postulated, that the "snowflake" texture is a result of the digestion of the original ignimbrite texture before final crystallization.

The SiO_2 percentage of the matrix was determined using the relationship between SiO_2 content and the index of refraction of the glass in the matrix (Williams, Turner, and Gilbert, 1954). The SiO_2 content ranges from 57.5 percent to 77.0 percent with an average of 61.18 percent (see Table 3).

The percent of matrix ranged from 75.96 percent to 91.41 percent; the average being 83.61 percent.

EXPLANATION OF TABLE 3

Percent SiO_2 in glass of matrix by index of refraction.

TABLE 3

Percent SiO_2 in glass of matrix by index of refraction*

Sample	Index (n)	Wt. % SiO_2
R-9-T	1.523	61.3
R-10-T	1.528	59.3
R-11-T	1.530	59.5
R-24-T	1.532	58.5
R-49-T	1.5225	62.5
R-23-T	1.529	59.2
R-94.25 Tb	1.519	63.5
R-102-Tb	1.532	58.5
R-117-Tb	1.509	68.0
R-115.1-Tb	1.529	59.2
R-115.2-Tb	1.527	60.0
R-149b-Tb	1.529	59.2
R-149u-Tb	1.528	59.5
R-149m-Tb	1.529	59.2
R-156.1-Tb	1.531	58.7
R-156.4-Tb	1.535	57.5
R-156.5-Tb	1.521	62.5
R-156.6-Tb	1.487	77.0
R-161-Tb	1.527	59.3
Mean		61.18

*Williams, Turner and Gilbert (1955)

CHEMICAL ANALYSIS OF THE BRITE IGNIMBRITE

One of the major objectives of this investigation was to analyze the 20 available samples of the Brite Ignimbrites using X-ray spectrography, flame photometry and analytical chemistry.

SiO_2, Al_2O_3, K_2O, CaO and total Fe (Fe^{++} and Fe^{+++}) were analysed by X-ray spectrography, Na_2O by flame photometry and FeO by analytical chemistry. The results are summarized in Tables 4 and 5.

SiO_2 Content

The SiO_2 content ranges from 59.50 percent to 83.00 percent with a mean of 74.11 percent. Except for two samples (R-115.2-Tb and R-156.5-Tb), all concentrations of SiO_2 are greater than 71 percent.

Al_2O_3 Content

Al_2O_3 ranges from 4.38 percent to 13.62 percent; the average Al_2O_3 is 9.22 percent. Except for one sample (R-156.6-Tb) all of the Al_2O_3 content appears to be contained in the feldspars. Sample R-156.6-Tb shows a small percentage of corundum in the norm calculations (see Table 6).

Fe_2O_3 Content

The Fe_2O_3 content was calculated by analyzing each sample for total Fe by X-ray spectrography and subtracting the amount of FeO as determined by analytical chemistry. The Fe_2O_3 content ranges from 1.17 percent to 4.45 percent; the average content is 2.03 percent.

Since most of the total Fe occurs as ferric ion, it seems reasonable to assume that it would appear in the sample as hematite. This assumption is confirmed by examination of the thin-sections and by the norm calculations.

EXPLANATION OF TABLE 4

Original chemical data.

TABLE 4

Original Chemical Data

Sample	R-9-T	R-10-T	R-11-T	R-14-T	R-23-T
SiO_2	80.13	81.28	82.75	76.82	83.81
Al_2O_3	9.07	8.71	8.06	10.45	7.17
Fe_2O_3	1.87	1.81	1.62	1.90	1.74
FeO	0.13	0.22	0.06	0.13	0.09
CaO	1.17	0.54	0.35	1.54	0.77
Na_2O	2.54	2.55	3.10	1.47	1.37
K_2O	5.10	4.89	4.07	7.68	5.05
Total	100.01	100.00	100.01	99.99	100.00

Sample	R-24-T	R-49-T	R-94.25-Tb	R-102-Tb	R-115.1-Tb
SiO_2	82.77	77.54	77.95	84.93	73.49
Al_2O_3	7.08	10.23	10.75	5.73	11.59
Fe_2O_3	1.74	2.35	2.21	1.57	2.81
FeO	0.12	0.10	0.20	0.10	0.08
CaO	2.51	0.62	0.92	1.52	1.96
Na_2O	2.37	4.21	2.71	2.43	3.59
K_2O	4.51	4.94	5.27	3.71	6.48
Total	100.00	99.99	100.01	99.99	100.00

TABLE 4 (concl.)

Original Chemical Data

Sample	R-115.2-Tb	R-117-Tb	R-149b-Tb	R-149m-Tb	R-149u-Tb
SiO_2	66.59	79.00	75.50	75.12	74.54
Al_2O_3	15.24	8.38	11.43	11.66	11.57
Fe_2O_3	4.98	2.25	2.09	2.25	2.30
FeO	0.35	0.13	0.09	0.13	0.17
CaO	2.92	2.09	1.88	1.49	1.68
Na_2O	4.66	3.85	2.93	3.58	3.62
K_2O	5.26	4.30	6.08	5.77	6.12
Total	100.00	100.00	100.00	100.00	100.00

Sample	R-156.1-Tb	R-156.4-Tb	R-156.5-Tb	R-156.6-Tb	R-161-Tb
SiO_2	75.75	74.89	70.72	83.97	72.71
Al_2O_3	12.14	11.52	5.02	7.96	9.34
Fe_2O_3	2.37	1.94	1.34	1.80	1.77
FeO	0.08	0.11	0.03	0.05	0.05
CaO	0.42	2.15	17.50	0.77	2.42
Na_2O	4.33	4.53	2.29	2.27	6.60
K_2O	4.91	4.86	3.08	3.16	7.10
Total	100.00	100.00	99.98	99.98	99.99

EXPLANATION OF TABLE 5

Normalized chemical data.

TABLE 5

Normalized Chemical Data

Sample	R-9-T	R-10-T	R-11-T	R-14-T	R-23-T
SiO_2	80.13	81.09	82.75	76.82	83.81
Al_2O_3	9.07	8.71	8.06	10.15	7.17
Fe_2O_3	1.87	1.81	1.62	1.90	1.74
FeO	0.13	0.12	0.05	0.13	0.09
CaO	1.17	0.54	0.35	1.54	0.77
Na_2O	2.54	2.55	3.10	1.47	1.37
K_2O	5.10	4.89	4.07	7.68	5.05
Total	100.01	100.00	100.01	99.99	100.00

Sample	R-24-T	R-49-T	R-94.25-Tb	R-102-Tb	R-115.6-Tb
SiO_2	82.77	77.54	77.95	84.93	73.49
Al_2O_3	7.08	10.23	15.75	5.73	11.59
Fe_2O_3	1.74	2.35	2.21	1.57	2.81
FeO	0.12	0.10	0.20	0.10	0.08
CaO	1.41	0.62	0.92	1.52	1.96
Na_2O	2.37	4.21	2.71	2.43	3.59
K_2O	4.51	4.94	5.27	3.71	6.48
Total	100.00	99.99	100.01	99.99	100.00

TABLE 5 (concl.)

Normalized Chemical Data

Sample	R-115.2-Tb	R-117-Tb	R-149b-Tb	R-149m-Tb	R-149u-Tb
SiO_2	66.59	79.00	75.50	75.12	74.54
Al_2O_3	15.24	8.38	11.43	11.66	11.57
Fe_2O_3	4.98	2.25	2.09	2.25	2.30
FeO	0.35	0.13	0.09	0.13	0.17
CaO	2.92	2.09	1.88	1.49	1.68
Na_2O	4.66	3.85	2.93	3.58	3.62
K_2O	5.26	4.30	6.08	5.77	6.12
Total	100.00	100.00	100.00	100.00	100.00

Sample	R-156.1-Tb	R-156.4-Tb	R-156.5-Tb	R-156.6-Tb	R-161-Tb
SiO_2	75.75	74.89	70.72	83.97	72.71
Al_2O_3	12.14	11.52	5.02	7.96	9.34
Fe_2O_3	2.37	1.94	1.34	1.80	1.77
FeO	0.08	0.11	0.03	0.05	0.05
CaO	0.42	2.15	17.50	0.77	2.42
Na_2O	4.33	4.53	2.29	2.27	7.60
K_2O	4.91	4.86	3.08	3.16	7.10
Total	100.00	100.00	99.08	99.98	99.99

EXPLANATION OF TABLE 6

Niggli molecular normative data.

TABLE 6

Niggli Molecular Normative Data*

Sample	R-9-T	R-10-T	R-11-T	R-14-T	R-23-T	R-24-T
Qt	44.43	46.37	50.68	37.10	54.99	53.27
Or	31.40	29.85	25.00	47.05	31.10	27.85
Ab	19.90	19.25	20.55	12.10	9.90	12.45
Σ Salic	95.73	95.47	96.23	96.25	95.99	93.57
Ac	3.00	3.44	1.68	1.16	2.32	4.16
Mt	0.36	0.51	0.00	0.36	0.18	0.58
Ht	0.34	0.12	0.76	0.85	0.58	0.00
Wo	0.58	0.46	0.38	1.38	0.94	1.04
Ap			0.16			
IL			0.24			
En			0.58			
Co						
Σ femic	4.28	4.53	3.80	3.75	4.02	5.56
Excess Na						

TABLE 6 (cont.)

Niggli Molecular Normative Data*

Sample	R-49-T	R-94.25-Tb	R-102-Tb	R-115.1-Tb	R-115.2-Tb
Qt	35.64	40.34	60.19	26.73	15.17
Or	29.70	32.20	23.00	39.20	31.55
Ab	27.10	25.00	9.60	25.25	42.30
An					5.20
Σ Salic	92.44	97.54	92.79	91.18	94.22
Ac	6.08	0.00	4.16	6.16	0.00
Mt	0.18	0.51	0.18	0.18	0.84
Ht	0.00	1.27	0.00	0.33	2.93
Wo	0.56	0.00	1.28	2.16	2.02
Ap					
IL					
En					
Co		0.69			
Σ femic	6.82	2.47	5.62	8.83	5.79
Excess Na	0.75		1.58		

TABLE 6 (cont.)

Niggli Molecular Normative Data*

Sample	R-117-Tb	R-149b-Tb	R-149m-Tb	R-149u-Tb	R-156.1-Tb
Qt	43.26	32.42	30.26	28.80	30.09
Or	26.05	36.85	34.95	36.90	29.25
Ab	20.90	27.10	30.10	27.55	37.70
An					
Σ Salic	90.21	96.37	95.51	93.25	97.04
Ac	5.52	0.04	2.04	4.52	1.32
Mt	0.33	0.18	0.33	0.33	0.18
Ht	0.00	1.34	0.86	0.30	1.24
Wo	2.40	2.06	1.26	1.60	0.22
Ap					
Il					
En					
Co					
Σ femic	8.25	3.62	4.49	6.75	2.96
Excess Na	1.54				

TABLE 6 (concl.)

Niggli Molecular Normative Data*

Sample	R-156.4-Tb	R-156.5-Tb	R-156.6-Tb	R-161-Tb	Mean
Qt	29.21	32.01	56.03	32.95	39.01
Or	29.40	19.05	19.40	41.75	31.08
Ab	34.65	9.25	21.10	8.85	22.03
An			1.15		0.32
Σ Salic	93.26	60.31	97.68	83.55	92.43
Ac	4.64	3.92	0.00	4.40	2.93
Mt	0.21	0.00	0.18	0.18	0.28
Ht	0.04	0.00	1.21	0.00	0.61
Wo	0.82	34.32	0.46	2.98	2.85
Ap					0.16
IL	0.34				0.03
En	0.70				0.06
Co			0.47		0.06
Σ femic	6.75	38.24	2.32	7.56	6.82
Excess Na		1.44		8.90	0.71

*Reference: Barth (1962).

It is possible (not investigated) that some of the iron could occur in the silicate structures as an Fe feldspar molecule (Bailey, 1964).

FeO Content

The FeO content as determined by analytical chemistry (see Table 7) is only in trace amounts ranging from 0.03 percent to 0.31 percent; the average is 0.12 percent. All FeO in the samples is probably contained in magnetite, which is partly or wholly altered to hematite.

CaO Content

The CaO content is ambiguous in at least several of the samples because of secondary calcite (in quantities up to at least 3 percent).

The CaO content ranges from 0.34 percent to 15.27 percent; the average is 2.04 percent. Only one sample (R-156.5-Tb) has a CaO content greater than 2.5 percent.

Na_2O Content

The Na_2O composition was determined by flame photometry and ranges from 1.36 percent to 6.60 percent; the average is 3.11 percent. The presence of excess Na_2O in the norm calculations indicate that at least a few of the samples are unusually high in Na_2O. The presence of this excess Na_2O is reflected in the diffraction patterns of several samples where anorthoclase appears in varying amounts.

K_2O Content

The K_2O content is completely incorporated in the alkali feldspars and ranges from 2.69 percent to 7.57 percent; the average is 4.91 percent. The K_2O content was determined by X-ray spectrograph and flame photometry (see

EXPLANATION OF TABLE 7

Titration data for FeO.

TABLE 7

Titration Data for FeO*

Sample	Wt. % FeO	Wt. % FeO (corrected)**
R-9-T	0.110	0.12
R-10-T	0.203	0.21
R-11-T	0.054	0.06
R-14-T	0.128	0.13
R-23-T	0.090	0.09
R-24-T	0.117	0.12
R-49-T	0.092	0.10
R-94.25-Tb	0.171	0.18
R-102-Tb	0.092	0.10
R-115.1-Tb	0.081	0.08
R-115.2-Tb	0.297	0.31
R-117-Tb	0.108	0.12
R-149b-Tb	0.090	0.09
R-149m-Tb	0.131	0.13
R-149u-Tb	0.153	0.16
R-156.1-Tb	0.072	0.08
R-156.4-Tb	0.107	0.11
R-156.5-Tb	0.029	0.03
R-156.6-Tb	0.052	0.05
R-161-Tb	0.047	0.05
G-1	0.090	0.94
W-1	8.495	8.86
R-3u-Tbr	0.216	0.23
R-4-Tba	4.160	4.32
$R\text{-}27\text{-}Tb_R$	0.491	0.51

*Peck (1964).

**Corrected from curves of Figure 2b.

Tables 1, 4 and 5).

The chemical analyses in this study carry an approximate maximum error of ± 5 percent.

DISCUSSION

Ignimbrites have been sporadically studied for many years by several methods; these studies have only resulted in isolated and incomplete theories as to the modes of formation for ignimbrites. Most of the theories and conclusions drawn from all previous investigations will at best apply only to a specific situation (Ross and Smith, 1960).

In all previous investigations, ignimbrites have usually been subjected to a combination of two modes of analysis. One method common to all of the investigations is petrography; especially universal stage studies. In addition, flame photometry, X-ray methods and analytical chemistry have been employed. First, however, the more fundamental features of ignimbrites should be discussed.

The mode of eruption, emplacement and crystallization history remain open to speculation. Ignimbrites are reported to have been erupted from both craters and fissures due to explosive and non-explosive events. The manner of emplacement has been variously described as of the nuee ardente type or as a flow of low viscosity, gas-charged lava.

Ignimbrites are rocks transitional and intermediate between tuffs and lavas (Vlodavetz, 1961), or else they may be equivalent to granite plutons that have been extruded (Ustiyev, 1961). Before accepting either of these two theories it will be necessary to carefully note the geologic features, petrography and chemical data associated with each individual ignimbrite body.

Ross and Smith (1960) stated,

> A principal characteristic of ash-flow tuffs is their common occurrence in thick units (tens of feet) of typically nonsorted or nonbedded materials. The most important single criterion for

recognition of the pyroclastic nature of ash-flow tuffs in the field seems to be the presence of pumic fragments.

> Ash-flow tuffs commonly show a wide range in size and relative amounts of constituent materials. The dominant material is generally ash or fine ash (4mm diameter) although some types are composed predominantly of pumic lapilli or blocks of different sizes, and for these latter types the term "pumice flow" may be more suitable than ash-flow.
>
> Many tuffs show a wide range in the proportion of anorthite in the plagioclase crystals and the more calcic ones are alien materials. The more calcic grains have tended to be out of equilibrium with their host rock and suffered alteration or resolution.

The entire rock may be much more silicic than suggested (Ross and Smith, 1960) from the groundmass if the bulk composition is not studied.

The misconception of low silica, which might lead to classification of these rocks as andesites, can result from an analysis of the groundmass (by index of refraction) without taking into consideration the enclosed phenocrysts. This appears to be indicated by, and helps to explain, the low silica percentage (60% SiO_2 by weight) in the groundmass (see Table 3).

Smith (1960) stated,

> In silicic welded tuffs granophyric crystallization is characterized by groundmass quartz intergrown with, or as blebs associated with, alkali feldspar and minor accessory minerals. The aggregate shows granophyric or micrographic textures similar to those shown by many slowly cooled rhyolitic flows, domes, and shallow intrusive rocks.
>
> Granophyric crystallization (quartz) has never been seen by the writer in fresh unaltered welded tuffs that were less than 600 feet thick. However, many older deposits and ultimately all deposits will probably contain quartz as the ground mass silica mineral, through conversion of cristobalite and tridymite.
>
> In rhyolitic tuffs, devitrification consists of the simultaneous crystallization of cristobalite and alkali feldspar to form submicroscopic spherulitic and axiolitic intergrowths of these minerals plus minor accessory minerals. This devitrification process is confined within shards or glass masses, whereas crystallization by growth of crystals into pore

spaces is a different process, related to the movement of vapors and transfer of material. Without pore space, vapor-phase crystallization cannot take place.

Several samples exhibit varying degrees of devitrification in glass masses and most of them also possess a "snowflake" texture in the matrix. This "snowflake" texture of the matrix appears to be superimposed on former devitrified structures. Evidence of this can be seen in Fig. 8 where relict structures of the pre-existing rock fragments are apparent. The "snowflake" texture is evidently a secondary feature in the evolution of the matrix.

Tuttle and Bowen (1958) present evidence that plagioclase phenocrysts will react with the liquid, eventually forming a single alkalic feldspar; although plagioclase and alkali feldspars are present in the early stages of crystallization.

The reacting of the plagioclase with the liquid soon after deposition, while the matrix is at a sufficiently elevated temperature to allow some mobility, could result in the digestion of the pre-existing ignimbrite texture and account for the presence of the finely disseminated secondary calcite. The calcite is present in all samples to some degree, and almost always is only seen associated with the groundmass. No vein calcite was observed in thin-section. With plagioclase reacting with the solution, quite possibly enough calcium ions would be available to form calcite, especially if enough CO_2 were made available through fumarolic activity or as a gas-streaming effect.

Although calcium ions normally tend to show an affinity for silicate structures, it is offset by the plagioclase reacting with the liquid, lowering temperature, and mobility of the CO_2 gas throughout the system.

Various zones of welding occur within each ignimbrite (Ross and

EXPLANATION OF FIGURE 8

Photomicrograph of Ignimbrite showing relict structures of pre-existing texture.

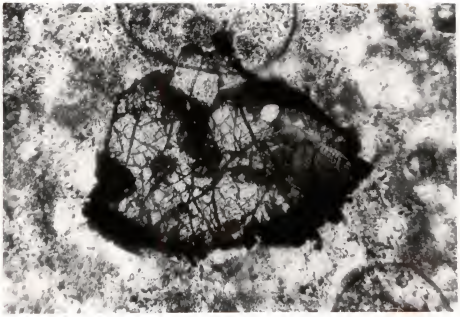

Figure 8

Smith, 1960). These are (from the upper and lower boundaries toward the center), the zone of no welding, the zone of partial welding, and the zone of dense welding. The presence and degree of welding in the various zones is dependent on the rate of cooling, temperature at time of emplacement, composition of the material extruded, rapidity of emplacement and the distance from its respective vent center.

The Brite Ignimbrite appears to be only a single member from a more complex eruptive unit. This may well apply to all other ignimbrites. Vlodavetz (1961) states that ignimbrite rocks commonly form a single rock unit with loose material and sintered tuff at the bottom which is overlain by a sequence of ignimbrite, welded tuff, nonwelded (compact) tuff, and unconsolidated, heterogeneous deposits at the surface.

Ignimbrites probably originate from numerous hot ash flows erupted in rapid succession from an anatectic magma saturated with gases during the post-orogenic stage of mountain building (Vlodavetz, 1961).

The distance from the vent and rapidity of emplacement affect the rate of cooling and the temperature of emplacement. The composition of the lava can be affected by the distance from a vent due to magmatic differentiation and/or assimilation. The vents for the Brite Ignimbrite are probably associated with deep-seated tectonic activity of the fissure type, and numerous vents are probably responsible for each flow. Therefore, little differences in chemical composition due to magmatic differentiation and/or assimilation can be observed.

Differences within the respective zones of welding, after crystallization, should be reflected in the analytical data providing care is exercised in the original sampling program. For future study, it is recommended that

at least one sample from each zone of welding at each location be collected and its relationship carefully noted.

Also, the consideration of each distinct flow unit as a separate eruptive event appears to be in error. Therefore, prior to a complete understanding of the ignimbrite process the underlying and overlying extrusive units must be studied and correlated with the unit in question.

CONCLUSION

It was hoped that some specific and useful knowledge on ignimbrites could be obtained through the use of numerous analytical techniques, although no broad geologic interpretations were intended. However, certain inferences seem valid from the data collected.

The following conclusions apply specifically to the Brite Ignimbrite, but may also apply to equivalent rocks throughout the world.

X-ray spectrographic analyses for some of the major constituents: SiO_2, Al_2O_3, total Fe, K_2O and CaO are rapidly obtained within acceptable limits of error (± 5% or less) when compared with standard analytical chemical methods.

Na_2O is best determined by flame photometry because the X-ray spectrographic methods are not yet refined enough for precise and accurate replicate analyses for this element. This method is reproducible to ± 3 percent for Na_2O.

FeO determinations are best carried out by the method described by Peck (1964). Careful attention to procedure allows an error of less than ± 2 percent.

During the early stages of this investigation an attempt was made to determine the composition of the feldspars using the universal stage method described by Haff (1942). No definite information was obtained due to the difficulty in obtaining extinction angles.

Although the samples were analyzed for only six of the major elements, except for two samples, these six elements comprise over 91 weight percent of the bulk composition (see Table 4).

The difference between the computed weight percent of each sample and

one hundred percent bulk composition is attributed to the presence of minor amounts of Ti, Mg, and CO_2. Future studies should include these elements plus as many others as feasible, especially Rb and Sr. The K/Rb and Ca/Sr ratio could be indicative of the stage of magmatic differentiation (Goldschmidt, 1962).

Each sample was examined qualitatively by X-ray diffraction to determine its mineralogical composition. The feldspars appear to form a solid solution series of X-ray perthites consisting of sanidine and anorthoclase with minor amounts of anorthite present in a few samples.

The data obtained by point counting (Chayes, 1956; see Table 2) were plotted on a ternary diagram as normative Qt-Or-Ab to determine if any correlation between ignimbrites and the melting minimum of granites (Tuttle and Bowen, 1958) could be established. The data did not yield a systematic distribution of points. This, in part, could be due to the presence of calcite in the samples and/or more probably indicates the affect of assimilation of wall rock material during eruption.

The petrographic studies indicate that no zone of dense welding is present in the Brite Ignimbrite. The lack of a zone of dense welding indicates low temperature of extrusion and a rapid rate of cooling.

Although no petrogenetic statements concerning ignimbrites can be made at this time, this study shows that such rocks are easily analyzed by the rapid techniques developed and tested in this thesis. The rapidity and accuracy of these methods should prove to be an extremely useful aid in geochemical research on ignimbrites in the future.

REFERENCES CITED

Bailey, D. K. and Schairer, J. F., 1964, The Peralkaline Residua System: Na_2O-Al_2O_3-Fe_2O_3-SiO_2: Car. Inst. Ann. Rept. of the Geop. Lab. Yrbk. 63, p. 74-79.

Barth, T. F. W., 1962, Theoretical Petrology: John Wiley and Sons, Inc., 416 p.

Birks, L. S., 1964, X-ray Spectrochemical Analysis, Vol. XI: John Wiley and Sons, Inc., New York, 137 p.

Chayes, F., 1956, Petrographic Modal Analysis: John Wiley and Sons, Inc., New York, 113 p.

Deford, R. K., 1958, Tertiary formations of Rim Rock Country, Presidio County, Trans-Pecos, Texas: Texas Jour. Sci., vol. 10, p. 1-37. (Reprinted as Univ. Texas Bur. Econ. Geol. Rept. inv. No. 9).

Erickson, R. L., 1953, Tascotal Mesa Quadrangle, Texas: Geol. Soc. America Bull., v. 64, No. 12, part 1, p. 1352-1371.

Fairbairn, H. W., Progress Report on Determination of Rb/Sr Ratios by X-ray Flourescence: Fourteenth Ann. Progress Rept. for 1966, Dept. of Geology and Geophysics, M.I.T., Cambridge, p. 187-191.

Goldschmidt, V. M., 1962, Geochemistry: Clarendon Press, Oxford, 733 p.

Haff, J. C., 1942, Fedorow Method (Universal Stage) of Indicatrix Orientation: Colorado School of Mines Quarterly, v. 37, No. 3, Golden, p. 1-28.

Klug, H. P. and Alexander, L. E., 1954, X-ray Diffraction Procedures: John Wiley and Sons, Inc., New York, 726 p.

Norelco X-ray Analytical Instrumentation, 1963, 59 p.

Peck, L. C., 1964, Systematic Analysis of Silicates: Geol. Sur. Bull. 1170, U. S. Government Printing Office, Washington, D. C., p. 72-73, 85-86.

Ross, C. S. and Smith, R. L., 1960, Ash-Flow Tuffs: Their Origin Geologic Relations and Identification: Geol. Sur. Prof. Paper 366, U. S. Government Printing Office, Washington, D. C., 81 p.

Smales, A. A. and Wager, L. R., 1960, Methods in Geochemistry: Interscience Publishers, New York, 464 p.

Smith, R. L., 1960, Zones and Zonal Variations in Welded Ash Flows: Geol. Sur. Prof. Paper 354-F, U. S. Government Printing Office, Washington, D. C., p. 149-159.

Tuttle, O. F. and Bowen, N. L., 1958, Origin of Granite in the Light of Experimental Studies in the System $NaAlSi_3O_8$-$KAl\ Si_3O_8$-SiO_2-H_2O: Geol. Soc. Amer. Mem. 74, 153 p.

Twiss, P. C., 1959, Geology of Van Horn Mountains, Trans-Pecos, Texas, Unpublished Ph. D. dissertation Univ. of Texas, Austin 234 p.

Ustiyev, E. K., 1961, Petrologic and Geologic Problems Related to Ignimbrites: in Tufflavas and Ignimbrites, A Survey of Soviet Studies, 1966, E. F. Cook ed. 212 p.

Vlodavetz, V. I., 1962, The Problems of Tufflavas and Ignimbrites: in Tufflavas and Ignimbrites, A Survey of Soviet Studies, 1966, E. F. Cook ed., 212 p.

Williams, H., Turner, F. J., and Gilbert, C. M., 1955, Petrography: W. H. Freeman and Company, San Francisco, 406 p.

ACKNOWLEDGMENTS

Thanks are expressed to Dr. Douglas G. Brookins for his supervision of this thesis. His assistance and helpful suggestions are gratefully acknowledged.

The writer also wants to thank Dr. Page C. Twiss, who introduced the writer to this study, and made available the samples used in this investigation.

Special thanks are due to Dr. J. R. Chelikowsky, Dr. C. W. Shenkel, and Dr. H. C. Fryer, committee members, for reading the manuscript of this thesis.

Graduate Teaching and Research assistantships made it possible for the writer to study at Kansas State University.

To all others, who helped during this investigation, the writer is thankful.

APPENDIX

X-ray Tube Selection

A general rule for selection of the most efficient X-ray tube is given as follows: The absorption edge of the X-ray target should be equal to, or slightly smaller, than the element to be analyzed. In general, for greatest efficiency, this demands that the X-ray target material be at least two atomic numbers higher than that of the element to be analyzed. The closer the X-ray target materials' absorption edge is to that of the element to be analyzed, the higher the peak intensity of that element.

Crystal Selection

In the early stages of an investigation using the X-ray spectrograph, it is desirous to qualitatively establish the elemental composition before attempting quantitative analysis. For this purpose, it is recommended that the operator select the LiF crystal to scan for those elements of atomic number 22(Ti) and higher and the PET crystal for elements from atomic number 13(Al) to atomic number 21(Sc). To date, it is not feasible to analyze for any element of atomic number 13 or less using the X-ray spectrograph. Future modifications on the instrument may allow the analysis of Na and Mg, however.

For detailed, quantitative analysis, the LiF crystal is best for those elements within its range and likewise for the PET crystal.

Special interest in certain elements (i.e. Rb and Sr) which have closely spaced peaks may require the use of specialized crystals. The Topaz crystal increases the peak to peak distance in Z between each element with a corresponding reduction in peak intensity. The spectral resolution increases as the d spacing of the analyzing crystal decreases.

EXPLANATION OF TABLE 8

Table of analyzing crystals.

TABLE 8

Table of Analyzing Crystals*

Analyzing Crystal	Lowest At. Number	Comments
Lithium Flouride (LiF)	Potassium K(19)	Optimum crystal for elements from Potassium to Uranium unless interfering peaks are present or additional separation of neighboring peaks is needed.
Ethylene diamine d Tartrate (EDDT)	Aluminum Al(13)	Used for Silicon and Aluminum in all matrices and Phosphorus, Sulphur, and Chlorine in intermediate and heavy element matrices. Crystal produces low background levels, for it contains no elements capable of X-ray flouresence by the incident beam.
Topaz	Titanium Ti(22)	High spectral resolution crystal. Used to minimize neighboring element peaks. Lower peak intensity than LiF.
Ammonium di-hydrogen Phosphate (ADP)	Magnesium Mg(12)	Optimum crystal for Magnesium. High background from Phosphorus flourescence in the crystal itself. Used for Magnesium only.
Calcium Sulphate (Gypsum)	Sodium Na(11)	Optimum crystal for Sodium. Can be used for Magnesium, Aluminum, Silicon, Phosphorus, Sulphur, and Chlorine. High flourescence background from Sulphur and Calcium in the crystal.
Pentaerythritol (PET)	Aluminum Al(13)	Optimum crystal for Aluminum, Silicon, Phosphorus, and Sulphur giving intensity increases from 1.4 to 1.9 depending on the matrix. Background levels same as EDDT.

*From: Norelco X-ray Analytical Instrumentation (1963).

EXPLANATION OF TABLE 9

Table of K peak angles.

TABLE 9

X-ray Spectrographic Specifications

Element	Order	Crystal			
		Topaz	LiF	PET	EDDT
			K peak angles in 2θ		
K	1		118.06	46.54	46.18
Ca	1		100.18	41.40	41.06
Ti	1	135.92	77.23	33.42	33.16
Cr	1	100.48	62.33	27.60	27.42
Fe	1	80.74	51.71	23.18	23.00
	2		121.42		
W	1	7.80			2.40

EXPLANATION OF TABLE 10

Table of K peak angles.

TABLE 10

X-ray Spectrographic Specifications

Element	Order	Crystal					
		Topaz	LiF	PET	EDDT	ADP	Gypsum
			K	peak angles in $^{o}2\theta$			
Na	1						103.30
Mg	1					136.46	81.27
Al	1			145.00	142.36	113.08	66.60
Si	1			109.20	108.00	84.02	55.97
	2						139.63
P	1			89.50	88.66	70.62	47.82
	2						108.32
K	1		136.58	50.70	50.28	41.16	28.53
	2			117.77	116.36	89.32	59.07
	3						95.35
	4						160.67
Ca	1		113.02	45.20	44.84	36.78	25.57
	2			100.45	99.42	78.24	52.52
	3					142.34	83.17
	4						124.47
Ti	1		86.10	36.60	36.34	29.92	20.87
	2			77.97	77.26	62.18	42.47
	3			141.33	138.94	101.54	65.80
Cr	1	115.28	69.32	30.24	30.15	24.84	17.35
	2			63.18	62.68	50.98	35.12
	3			103.65	102.56	80.40	53.82
	4					118.76	74.23
	5						97.94
Mn	1	101.70	62.95	27.83	27.62	22.78	15.92
	2			57.52	57.04	46.54	32.17
Fe	1	91.18	57.50	25.62	25.42	20.96	14.67
	2		148.27	52.62	52.19	42.68	29.57
	3			83.33	82.58	66.14	45.00
	4			124.85	123.22		61.37
Rb	1	39.96			12.08	9.98	
Sr	1	37.72			11.42	9.44	
Mo	1	30.38	20.32	9.33	9.26	7.66	
	2	63.22	41.32	18.72	18.56	15.34	
	3	103.66	63.92	28.23	28.01	23.10	
	4		89.77	32.95	37.66	30.96	

TABLE 10 (concl.)

Element	Order	Crystal					
		Topaz	LiF	PET	EDDT	ADP	Gypsum
			K	peak angles in $^{o}2\theta$			
W	1	8.91			2.74	2.26	
	2	17.86			5.48	4.54	
	3	26.94			8.22	6.80	
	4	36.18			10.98	9.07	
	5	45.70			13.73		

EXPLANATION OF TABLE 11

Oxide analyses of standard rock powders.

TABLE 11

Oxide Analyses of Standard Rock Powders

Sample	R-4-Tba	R-156.8-Tpc	R-11-T	R-156.4-Tb	R-3U-Tbr
SiO_2	43.44	59.33	80.91	72.89	65.95
TiO_2	2.89	1.67	0.17	0.25	0.53
Al_2O_3	15.00	14.58	7.88	11.21	12.63
Fe_2O_3	7.81	3.48	1.57	1.88	5.71
FeO	4.42	3.62	0.07	0.02	0.27
MnO	0.17	0.15	0.07	0.11	0.16
MgO	5.91	2.09	0.20	0.23	0.07
CaO	10.04	3.99	0.34	2.09	2.15
Na_2O	3.70	4.57	2.40	4.32	4.46
K_2O	1.95	4.18	3.98	4.73	5.57
H_2O+	1.59	1.60	1.75	1.06	0.89
H_2O-	1.15	0.40	0.60	0.28	0.39
P_2O_5	1.26	0.74	0.04	0.02	0.08
CO_2	1.19	0.18	0.06	1.30	1.30
Total	100.52	100.59	100.04	100.49	100.16

TABLE 11 (cont.)

Sample	R-27-Tbr	R-157-Tp	R-41-Tp	R-113-Tby
SiO_2	70.46	67.92	66.85	72.82
TiO_2	0.47	0.49	0.62	0.34
Al_2O_3	11.67	13.52	14.11	10.81
Fe_2O_3	5.07	3.63	4.09	2.81
FeO	0.57	0.12	0.29	0.09
MnO	0.16	0.06	0.06	0.06
MgO	0.08	0.39	0.11	0.08
CaO	0.95	1.70	1.25	1.63
Na_2O	4.68	3.94	3.92	2.27
K_2O	4.92	5.56	5.20	6.29
H_2O+	0.63	1.18	1.96	1.28
H_2O-	0.29	0.71	0.76	0.35
P_2O_5	0.08	0.15	0.20	0.12
CO_2	0.17	0.55	0.03	0.72
Total	100.20	99.92	99.45	99.67

TABLE 11 (cont.)

Sample	R-140-Tby	AB 4	R-2	R-6
SiO_2	72.62	1.85	21.13	22.91
TiO_2	0.21	Tr	1.80	1.72
Al_2O_3	10.73	0.07	4.28	4.63
Fe_2O_3	2.55	0.11	7.44	6.80
FeO	0.16	0.15	1.79	2.94
MnO	0.05	0.04	0.22	0.14
MgO	0.15	0.74	20.04	20.36
CaO	2.54	53.51	18.62	16.68
Na_2O	2.98	0.05	0.27	0.51
K_2O	5.15	0.05	0.16	0.15
H_2O+	1.13	0.61	8.65	8.76
H_2O-	0.52	0.38	1.31	1.79
P_2O_5	0.02	0.07	1.39	1.19
CO_2	1.63	42.39	11.72	10.69
SrO		0.026	0.12 Cr_2O_3	0.12 Cr_2O_3
			0.34 SO_3	0.29 SO_3
Total	100.44	100.046	99.28	99.68

TABLE 11 (concl.)

Sample	G-1	W-1
SiO_2	72.52	52.58
TiO_2	0.26	1.08
Al_2O_3	14.08	14.94
Fe_2O_3	0.85	1.38
FeO	0.94	8.71
MnO	0.02	0.17
MgO	0.35	6.52
CaO	1.36	10.92
Na_2O	3.29	2.15
K_2O	5.52	0.63
H_2O+	0.25	0.45
H_2O-	0.02	0.08
P_2O_5	0.09	0.14
CO_2	0.08	0.07
Others	0.29	0.19
Total	99.93	100.02

Reagents and Solutions for the Determination of Ferrous Oxide

Dissolving solution. To prepare the dissolving solution, transfer 50 grams of boric acid to a 2-liter beaker; then add 1500 ml of demineralized water, 175 ml of sulfuric acid, and 200 ml of phosphoric acid. This mixture is then heated to dissolve the boric acid crystals. After the boric acid crystals are completely dissolved, cool the solution, transfer it to a polyethylene storage bottle and dilute to 2 liters.

Sodium diphenylamine sulfonate-0.2 percent. Dissolve 0.2 gram of sodium diphenylamine sulfonate in 100 ml of hot demineralized water.

Potassium dichromate-0.06262N at 25°C. This solution should be prepared with demineralized water at room temperature. Determine the temperature of the water with a thermometer and add 1 liter to a 2-liter flask. Calculate the amount of potassium dichromate required from the table below:

Temp. of Water (°C)	$K_2Cr_2O_7$ required (grams)	Temp. of Water (°C)	$K_2Cr_2O_7$ required (grams)
21	6.147	26	6.140
22	6.146	27	6.138
23	6.144	28	6.137
24	6.143	29	6.135
25	6.141	30	6.134

Weigh this amount of potassium dichromate and transfer it to the flask; swirl the flask until all of the potassium dichromate dissolves. Dilute this solution to 2 liters and mix.

PETROGRAPHY OF BRITE IGNIMBRITE, TRANS PECOS, TEXAS

by

JERRY P. SMITH

B. S., Kansas State College, 1959

AN ABSTRACT OF A MASTER'S THESIS

submitted in partial fulfillment of the

requirements for the degree

MASTER OF SCIENCE

Department of Geology and Geography

KANSAS STATE UNIVERSITY
Manhattan, Kansas

1967

The geochemistry of twenty samples from the Brite Ignimbrite of the Vieja Group of Tertiary Age in Trans Pecos Texas was investigated by X-ray spectrographic and diffraction methods, flame photometry, wet chemistry and petrography. The intention was to establish a basis for future study of the petrogenesis of ignimbrites. Each of the methods have proven useful in rapidly acquiring meaningful data.

The oxides SiO_2, Al_2O_3, total Fe, CaO and K_2O were determined by X-ray spectrography. Peak intensities were determined graphically using twelve commercially analyzed rock powders as standards. The ratio, counting and Fe_K methods were not used; but are discussed in the text as methods to be used when greater accuracy is required.

The flame photometer was used to analyze for Na_2O since the X-ray spectrograph can not be used for this oxide. K_2O was also determined by this method to check the accuracy of the X-ray spectrographic analyses.

Wet chemistry was utilized for the determination of ferrous iron and subtracted from the total iron to yield the ferric iron concentration.

Early in the investigation an attempt was made to determine the chemical composition of the feldspars by universal stage measurements. This was abandoned due to the difficulty in obtaining extinction angles for the feldspars due to their perthitic nature.

All of the methods utilized proved useful, except for the universal stage procedures, and the data demonstrate the usefulness of the analytical methods employed for the study of rocks of ignimbrite composition.

The variation in major element concentration in the samples studied is (in weight percent): SiO_2, 59.50 to 83.00; Al_2O_3, 4.38 to 13.62; Fe_2O_3, 1.17 to 4.45; FeO, 0.03 to 0.31; CaO, 0.34 to 15.27; Na_2O, 1.36 to 6.60 and

K_2O, 2.69 to 7.57.

The error for a single analysis is: SiO_2 ± 4.0 percent, Al_2O_3 ± 5.0 percent, total Fe ± 4.0 percent, FeO ± 2.0 percent, CaO ± 4.0 percent, Na_2O ± 3.0 percent, and K_2O ± 4.0 percent.

Twelve of the samples were studied by point counting to determine the normative mineral composition. This method did not appear to warrant further investigation at this time due to insufficient data for the samples and the fact that their locations within the formation are quite different.